ICSV 21
13-17 July, 2014, Beijing/China

The 21st International Congress on Sound and Vibration

13-17 July, 2014, Beijing/China

INFLUENCE OF THE SPATIAL PRIMARY FIELD PROPERTIES ON ACTIVE CONTROL PERFORMANCE

Stephen J. Elliott and Jordan Cheer

Institute of Sound and Vibration Research, University of Southampton, U.K.

e-mail: s.j.elliott@soton.ac.uk

A general formulation is presented of the optimum controller in an active system for local sound control in a spatially random primary field. The sound field in a control region is selectively attenuated using secondary sources, driven by reference sensors, all of which are potentially remote from this control region. It is shown that the optimal controller has the form of a remote microphone system, with a least-squares estimation of the disturbance signals in the control region from the reference signals. The sound field under control is assumed to be generated by an array of primary sources, whose source strengths are specified using a spectral density matrix. This can easily be used to synthesize a diffuse primary field, if the primary sources are uncorrelated and far from the control region, but can also generate primary fields dominated by contributions from a particular direction, for example, which is shown to significantly affect the shape of the resulting zone of quiet.

1. Introduction

Active sound control in enclosures works well at low frequencies, when the size of the enclosure is not too large compared with the acoustic wavelength[1]. At higher frequencies, however, when global control of the sound field cannot be achieved, local active control can still be used to reduce the sound in a particular region of space. Above the Schroeder frequency [2, 3] the sound field can often be approximated by a diffuse field, with equal energy incident from all directions. The zone of quiet, within which the original sound level is reduced by at least 10dB, that can be generated by a remote secondary source around a control microphone in a diffuse field has a diameter of about one tenth of an acoustic wavelength [4]. The secondary source cannot be too remote, however, since otherwise it can increase the sound level elsewhere in the enclosure[5], and so various arrangements of active control system with local secondary source, close to the control region have been investigated [6, 7, 8, 9, 10].

In the development of local active controllers there has also been considerable interest, for practical reasons, in monitoring the sound field within the region of control with sensors outside this region, as reviewed by Moreau *et al* [11.] Originally a "virtual microphone" technique was proposed for the problem [12, 13, 14, 15], where the primary pressure was assumed to be the same at the sensor and in the control region. Later, systems were developed using the "remote microphone" technique [16, 11], which assume a given transfer response between the sensor and control region.

There is thus an on-going interest in the performance of feedforward active control systems that generate local zones of quiet with secondary sources and sensors outside of the region of control. This paper presents a general formulation for the calculation of the performance of such systems. The formulation uses spectral density matrices [10] and the result is an expectation of the resulting mean square pressure in the region of control, which avoids the calculation of the multiple results that has previously been used for different realisations of the random primary field [17, 13]. The formulation also allows a general specification of the spatially random primary sound field, in terms of a distribution of energy from different angles, for example. It is shown that this significantly affects the results of some model calculations and that the conventional diffuse field assumption is not sufficient to predict the performance of local active control systems in such circumstances.

2. Formulation

An illustration of the physical arrangement assumed here is shown in Fig. 1. An array of primary sources, of source strengths $\boldsymbol{v}^T = [v_1, v_2 \dots v_{Nv}]$, is assumed to generate the spatially random pressure field under control. This field is detected by a set of reference sensors producing signals $\boldsymbol{x}^{\boldsymbol{T}} = [x_1, x_2 \dots x_{Nx}]$, which are used to drive a set of secondary sources with signals $\boldsymbol{u}^T = [u_1, u_2 \dots u_{Nu}]$. The region of control is assumed to be monitored by a set of sensors with outputs $\boldsymbol{y}^{\boldsymbol{T}} = [y_1, y_2 \dots y_{Ny}]$, some of which are used to define the cost function used in the design of the control system.

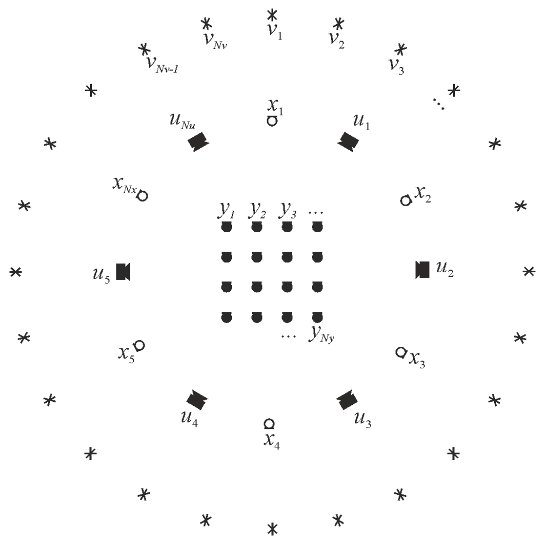

Figure 1. Illustration of the kind of geometeric arrangement assumed, in two dimensions in this case.

Although the arrangement illustrated in Fig. 1 is in two dimensions, the simulations below have been conducted with the primary sensors arranged on a spherical grid surrounding the local control system. It has also been assumed in this figure that the reference sensors and secondary sources are outside the region over which active control is to be implemented. The sound field in this region is monitored by a dense array of detection sensors, so that the sound field can be visualised, even though only some of the signals from these sensors are directly controlled. It has also been assumed in the simulations below that the transfer responses between the sources and sensors are those in a free field, although this assumption is not necessary.

In the formulation used here, all the signals are assumed to be about a single frequency and proportional to $e^{j\omega t}$, although this dependence on ω is suppressed for notational convenience. The signals are, however, assumed to be random variables, with their average proportions defined by spectral density matrices, as described, for example, in [10,1].The spectral density matrix defining the primary source strengths, for example, is given by

$$\boldsymbol{S}_{vv} = E[\boldsymbol{v}\boldsymbol{v}^H], \tag{1}$$

where the superscript ^{H} denotes the Hermitian, complex conjugate transpose and E denotes the expectation operator. The diagonal elements of $\boldsymbol{S}_{vv}$ are the power spectral densities of each individual primary source, and the off-diagonal terms are the cross spectral densities between these sources. It will be assumed in the simulations below that the primary sources are uncorrelated, so that $\boldsymbol{S}_{vv}$ is a diagonal matrix, although this is not necessary in the general formulation. The spectral density matrix could, for example, be used to define a spatially correlated pressure field [18] or a set of original primary sources and their image sources, to approximate an enclosed sound field [3].

The block diagram for the system is illustrated in Fig. 2, where the primary sources, $\boldsymbol{v}$, generate the reference signals, $\boldsymbol{x}$, and the disturbance signals at the monitoring sensors, $\boldsymbol{d}$, via the matrices of transfer responses $\boldsymbol{R}$ and $\boldsymbol{P}$ respectively. The matrix of transfer responses from the secondary sources, $\boldsymbol{u}$, to the monitoring sensors, $\boldsymbol{y}$, is denoted $\boldsymbol{G}$, but it is assumed that any feedback from the secondary sources to the reference sensors, $\boldsymbol{F}$, is cancelled out by a perfect model, $\widehat{\boldsymbol{F}}$ equal to $\boldsymbol{F}$, within the overall controller [10] as explicitly shown in Fig. 2.

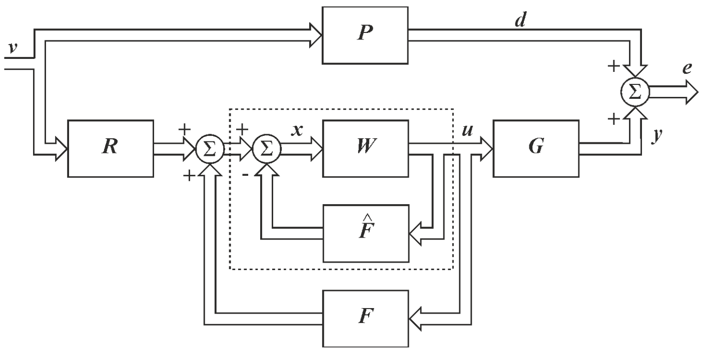

Figure 2. The block diagram of the assumed control system.

The matrix of control filters, $\boldsymbol{W}$, which drive the secondary sources from the reference sensors, is thus entirely feedforward. It may seem a little strange to have to detect the primary field when it is at a single frequency, but it must be remembered that this field is assumed here to be stochastic, rather than deterministic, as would be the case for a tonal controller, for example. The vector of signals at the monitoring sensors can thus be written as

$$\boldsymbol{e} = \boldsymbol{d} + \boldsymbol{G}\,\boldsymbol{W}\,\boldsymbol{x}. \tag{2}$$

The cost function to be minimised is a weighted sum of the modulus squared signal from the monitoring sensors, which can be written as

$$J = E\,[\boldsymbol{e}^H\,\boldsymbol{A}\,\boldsymbol{e}] = trace\,E[\boldsymbol{A}\,\boldsymbol{e}\,\boldsymbol{e}^H], \tag{3}$$

where $\boldsymbol{A}$ is a square Hermitian "aperture" matrix, through which the error signals to be minimized are selected from all the monitoring sensors. Although it is assumed in the simulations below, that $\boldsymbol{A}$ is a real, diagonal, matrix, and used to select the few monitoring signals to be minimised out of the whole array, for example, this assumption is not necessary in the general formulation.

The second form of the cost function in eq. (3) is written in terms of the trace of the spectral density matrix for $\boldsymbol{e}$[10]. In this form, the cost function can be expanded out using eq. (2) to give

$$J = trace\left[\boldsymbol{A}\,\boldsymbol{G}\,\boldsymbol{W}\,\boldsymbol{S}_{xx}\,\boldsymbol{W}^H\boldsymbol{G}^H + \boldsymbol{A}\,\boldsymbol{G}\,\boldsymbol{W}\,{\boldsymbol{S}_{xd}}^H + \boldsymbol{S}_{xd}\,\boldsymbol{W}^H\boldsymbol{G}^H\boldsymbol{A}^H + \boldsymbol{A}\boldsymbol{S}_{dd}\right], \tag{4}$$

where the spectral density matrix for the reference signals, and the cross spectral density matrix between the output of the reference and detection sensors, are defined to be

$$\boldsymbol{S}_{xx} = E\;[\boldsymbol{x}\,\boldsymbol{x}^H]\text{ and }\boldsymbol{S}_{xd} = E\,[\boldsymbol{d}\,\boldsymbol{x}^H] \tag{5}$$

The properties of the trace operator, that $trace\,(\boldsymbol{A}+\boldsymbol{B})$ is equal to $trace\,(\boldsymbol{A}) + trace\,(\boldsymbol{B})$ and that $trace\,(\boldsymbol{AB})$ is equal to $trace\,(\boldsymbol{BA})$, together with the fact that $\boldsymbol{A}$ is Hermitian, have also been used in the formulation of the third term in the right hand side of eq. (4).

A generalisation of the result derived in [10, 19] then allows the optimum set of control filters to be obtained that minimise the cost function in eq. (4), as

$$\boldsymbol{W}_{opt} = -[\boldsymbol{G}^H \boldsymbol{A}\boldsymbol{G}]^{-1}\, \boldsymbol{G}^H\, \boldsymbol{A}\, \boldsymbol{S}_{xd}\, \boldsymbol{S}_{xx}{}^{-\mathbf{1}}, \tag{6}$$

where it is assumed that both $\boldsymbol{G}^H\boldsymbol{A}\boldsymbol{G}$ and $\boldsymbol{S}_{xx}$ are invertible.

From the block diagram shown in Fig. 2, it can be seen that $\boldsymbol{x}$ is equal to $\boldsymbol{R}\boldsymbol{v}$, assuming that $\widehat{\boldsymbol{F}}$ is equal to $\boldsymbol{F}$, and that $\boldsymbol{d}$ is equal to $\boldsymbol{P}\boldsymbol{v}$, so that the matrices $\boldsymbol{S}_{xx}$ and $\boldsymbol{S}_{xd}$, as defined in eq. (5), are equal to

$$\boldsymbol{S}_{xx} = \boldsymbol{R}\, \boldsymbol{S}_{vv}\, \boldsymbol{R}^H, \text{ and } \boldsymbol{S}_{xd} = \boldsymbol{P}\, \boldsymbol{S}_{vv}\, \boldsymbol{R}^H, \tag{7}$$

where $\boldsymbol{S}_{vv}$ is the spectral density matrix of the primary source signals, as defined in eq. (1). The optimum matrix of control filters is thus equal to

$$\boldsymbol{W}_{opt} = -[\boldsymbol{G}^H \boldsymbol{A}\boldsymbol{G}]^{-1}\, \boldsymbol{G}^H\, \boldsymbol{A}\, \boldsymbol{P}\, \boldsymbol{S}_{vv}\, \boldsymbol{R}^H\, [\boldsymbol{R}\, \boldsymbol{S}_{vv}\, \boldsymbol{R}^H]^{-1}, \tag{9}$$

where the matrices of transfer responses $\boldsymbol{G}, \boldsymbol{R}$ and $\boldsymbol{P}$ are defined by the assumed geometry, $\boldsymbol{S}_{vv}$ is defined by the assumption of the primary field and $\boldsymbol{A}$ is determined by definition of the local field under control.

3. Simulations

A series of simulations is initially performed of control at a single position in a simulated diffuse primary sound field using a single monopole secondary source separated by a distance, L, equal to 0.1 m. 408 uncorrelated monopole sources uniformly distributed over a sphere of radius 1 m was used to generate the primary field. This resulted in the averaged spatial correlation function shown in Fig. 3 for the pressure in a 0.5 m $\times$ 0.5 m control region measured by a 51 $\times$ 51 grid of monitoring microphones, which is at the centre of the sphere. Also shown in Fig. 3 is the $\sin(kr)/\,kr$ theoretical form for this spatial correlation function [2, 4], where k is the wavenumber and r the separation distance between the two pressures, which shows very good agreement for values of kr up to about 25, which corresponds to a frequency of around 12.5 kHz in the simulations here if r is equal to the assumed separation, L, between the secondary loudspeaker and error microphone.

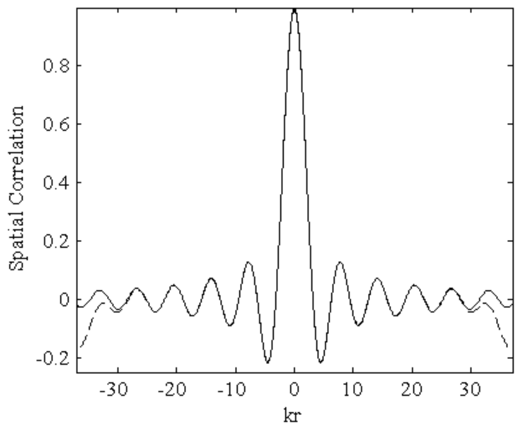

Figure 3. Spatial correlation function for the pressure obtained for simulations of a diffuse field, dashed line, and the theoretical value, solid line.

In these initial simulations the detection microphone is assumed to be collocated with the single error microphone at the centre of the sphere of primary sources. The spatial extent of the zone of quiet calculated from this simulation, within which the expectation of the primary pressure has been reduced by 10 dB, is shown in Fig. 4a for various normalized excitation frequencies. The normalized excitation frequency is expressed as kL where L is the separation distance between the secondary source and cancellation point. These results are very similar to the results of previous calculations of the zone of quiet [17] estimated by averaging multiple simulations, except that the zones of quiet are more symmetrical indicating a better estimate of the spatial extent of these zones.

Fig. 4b shows the results of cancelling at the same point, but with a reference sensor in the arrangement described in Section 2 half way between this point and the monopole secondary source thus implementing the remote microphone method. It can be seen that the results are similar to those of Fig. 4a when the wavelength is large compared with the separation distance between the reference and cancellation points, so that $kL/2$ is small compared with unity, but are degraded at higher normalised frequencies. For comparison, Fig. 4c shows the results of assuming that the primary field is the same at the reference and cancellation points, and only taking account of the difference between the deterministic secondary sound field at these points, as in the virtual microphone, [12, 13, 11] arrangement. It can be seen that there is little difference between these two approaches in this case.

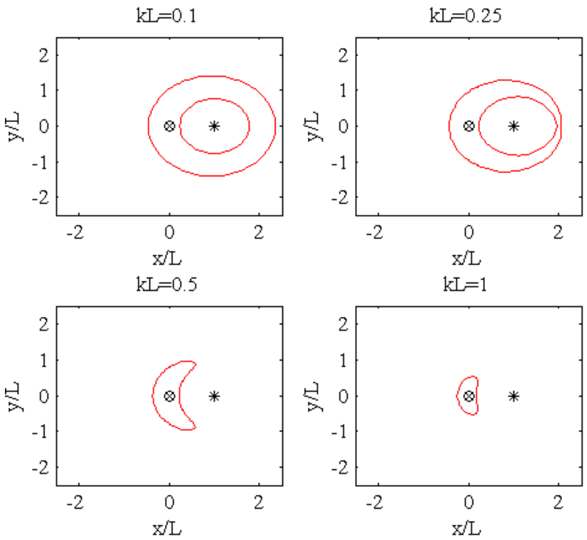

(a) Physical microphone at control point.

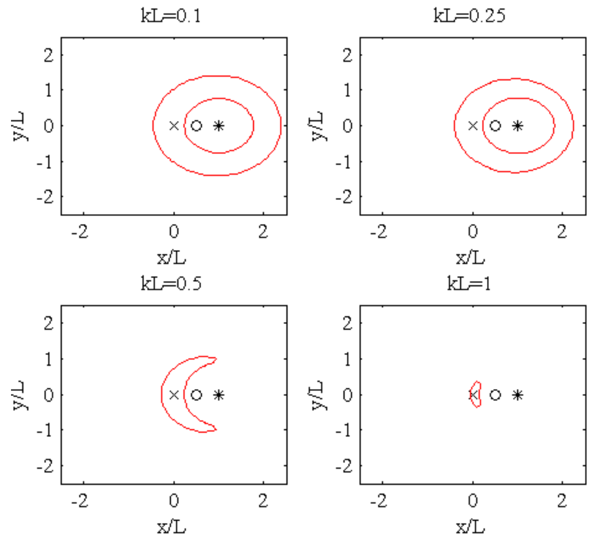

(b) Remote microphone method.

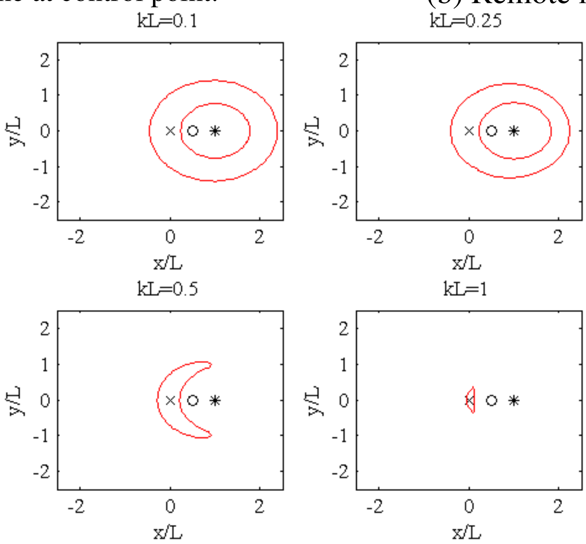

(c) Virtual microphone method.

Figure 4. Zone of quiet within which the average pressure is reduced by 10 dB from simulations of cancellation of a diffuse field at a single point, x, using a control sensor, o, and a single monopole secondary source, *, at four different normalised frequencies.

It should be emphasised that this result was obtained with a single calculation, as opposed to the average over multiple calculations that had previously been used to simulate such a field [4, 5, 13].

The performance of the three control strategies used in Fig. 4 are compared at different frequencies in Fig. 5. This shows the axial extent of the 10 dB zone of quiet, i.e. on a line from the secondary source location to the cancellation point, as a function of normalized excitation frequency, kL. Not surprisingly, the case in which a physical microphone can be placed at the cancellation point always performs best, but the remote microphone method, implied by the formulation used in section 3, and the simpler virtual microphone arrangement have a very similar performance for kL less than about 0.5.

The influence of the spatial distribution of the primary field on the shape of the zone of quiet is illustrated in Fig. 6, for the remote microphone method at a normalized excitation frequency of kL equal to 0.5. The shape of the zone of quiet for the simulations of the diffuse sound field is the same as that in Fig. 4b, but also shown in this figure is the shape of this zone when only 21 uncorrelated primary sources are operating, either above or to the right or to the left of the quiet zone. The zone of quiet is greatest when the primary field is mainly from above, since in this case the primary pressure field is almost uniform in the plane shown in Fig. 6, so that reductions at the control point will result in similar reductions at all positions which are a similar distance from the secondary source. The zone of quiet is also somewhat greater than that with a diffuse primary field when the primary field is mainly from the left, since the phase variation of the primary field then more nearly matches that of the secondary field. It is somewhat smaller than the diffuse field result when the primary field is mainly from the right, however, as the phase variations of the primary and secondary field then do not match.

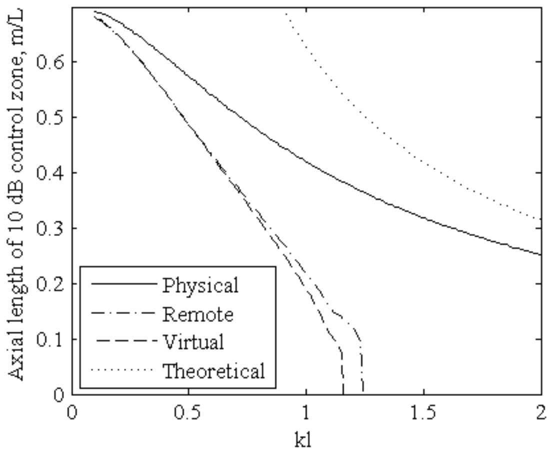

Figure 5. Axial length of 10 dB zone of quiet as a function of non-dimensional frequency for cancellation at a point a distance L from a monopole secondary source, solid line, the use of a virtual microphone at $L/2$, dashed line, the use of a remote microphone at $L/2$, dash-dotted line, and the theoretical λ/10 limit, dotted line.

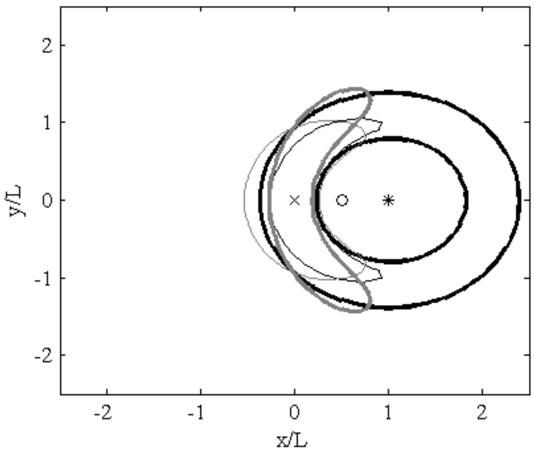

Figure 6. The extent of the 10 dB zone of quiet, for a normalized excitation frequency of $kL=0.5$, when the simulated field is a diffuse, thin solid black line, mainly coming from above, thick solid black line, mainly from the right hand side, thin solid grey line, and mainly from the left hand side, thick solid grey line.

Finally, the full power of the multichannel formulation is illustrated in Fig. 7, in which four monopole secondary sources, on a square of length, $L = 0.2$, are used to control the sum of the mean square pressures at 3 by 3 array of monitoring microphones centrally arranged in a square of length $L/2$.

It should be noted that since in this case the zone of quiet is significant up to higher frequencies, the results are shown for kL equal to 0.25, 0.5, 1 and 1.5 instead of 0.1, 0.25, 0.5 and 1 in the single channel results above. For values of kL below about 0.5, the zone of quiet extends around the secondary sources, except within the immediate vicinity of these sources, because of their near fields. The 10 dB zone of quiet does not extend beyond the secondary source for normalized excitation frequencies, kL, above about 1, but still encloses the reference sensors in this case.

The results in Fig. 7 are only shown within the plane of the secondary sources and reference sensors, however, the diameter of the zone of quiet created with this four channel system is about 0.6 λ, which is clearly significantly more than the upper limit of 0.1 λ generated by the single channel system. The shape of the zone of quiet will be affected in practice by the physical size of the secondary sources and by any non-uniform directivity of the primary field. The results in Fig. 7 do indicate, however, that zones of quiet that are significantly larger than the single λ/10 single channel limit are possible using local active control systems with only four secondary sources.

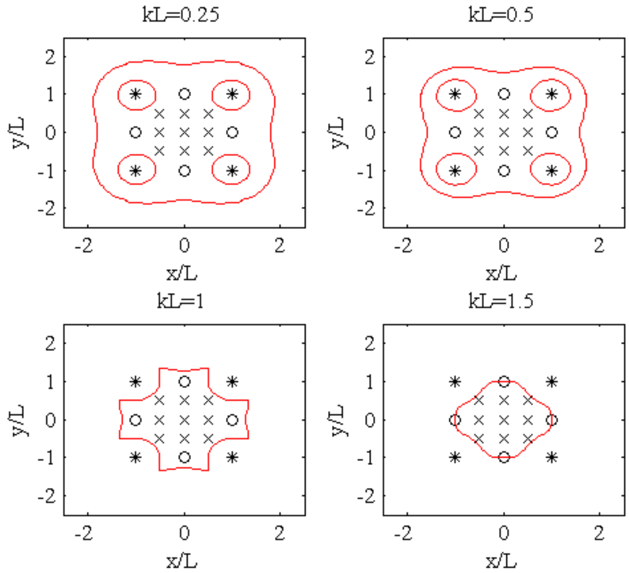

Figure 7. Extent of the 10 dB zone of quiet when four secondary sources are optimally driven from four reference sensors in a diffuse field simulation to generate a zone of quiet over the entire 3x3 array of monitoring microphones, x, using four secondary sources, *, and four control sensors, o, at various normalized excitation frequencies.

4. Conclusions

A general formulation has been presented for the optimal least-squares solution to the local active noise problem in a spatially random primary sound field. The field under control is assumed to be generated by an array of primary sources, specified in terms of their spectral density matrix. By assuming a uniform distribution of uncorrelated primary sources in the far field, a diffuse primary field is readily generated, but the formulation also allows more realistic primary fields to be generated, such as when it is dominated by sources in a particular direction, or in an enclosure.

By analyzing the adaptive version of this method it is shown that the optimum filter effectively implements a remote microphone technique. The form of this optimal solution is shown to consist of the generalized inverse of the plant matrix, from secondary source output to reference sensor input, and the least squares estimate of the disturbance field in the region of control, calculated from the outputs of an array of reference sensors that may be remote from this region.

By way of illustration, a number of simulations that use this optimal solution are then presented, starting with local control at a point in a diffuse primary field. It is seen how the present formulation provides a single closed-form solution to the expectation of the resulting field, rather than having to average the result over many realizations of the primary field, as had been done previously.

The influence of the spatial directivity of the primary field on shape of the zone of quiet is then explored, showing that it is important to take this directivity into account when predicting the performance of local active sound control systems. Finally, the results of a local active control system are calculated for the case of multiple secondary sources and multiple reference signals, all outside the zone of control, which demonstrate the generality of the solution.

REFERENCES

1. Nelson, P.A. and Elliott, S.J., 1992. *Active Control of Sound.* Academic Press.
2. Schroeder, M.R. and Kuttruff, K.H., 1962. On frequency response curves in rooms. *Journal of the Acoustical Society of America,* 34, 76-80.
3. Pierce, A.D., 1981. Acoustics: an introduction to its physical principles and applications. McGraw Hill.
4. Elliott, S.J. et al , 1988. Active cancellation at a point in a pure tone diffuse sound field. *Journal of Sound and Vibration,* 120 (1), 183-189.
5. Joseph, P. Elliott, S.J. and Nelson, P.A., 1994. Near Field Zones of Quiet. *Journal of Sound and Vibration,* 172 (5), 605-627.
6. Miyoshi, M., Shimizu, J. and Koizumi, N., 1994. On arrangements of noise-controlled points for producing larger quiet zones with multi-point active noise control. In: ASJ (Acoustical Society of Japan), *23rd Inter-Noise Congress.* Yokohama, Japan, 29-31 August 1994.
7. Hashimoto, H., Terai, K., Kiba, M. and Nakama, Y., 1995. Active noise control for the seat audio system. In: *Proceedings of the 1995 International Symposium on Active Control of Sound and Vibration (Active 95).* California, U.S.A., 06-08 July 1995.
8. Rafaely, B., Elliott, S.J. and Garcia Bonito, J., 1999. Broadband performance of an active headrest. *Journal of the Acoustical Society of America*, 106 (2), 787-793.
9. Olson, H.F. and May, E.G., 1953. Electronic Sound Absorber. *Journal of the Acoustical Society of America*, 25, 1130-1136.
10. Elliott, S.J., 2001. Signal Processing for Active Control. Academic Press.
11. Moreau, D., Cazzolato, B., Zander, A. and Petersen, C., 2008. A review of virtual sensing algorithms for active noise control. *Algorithms,* 1, 69-99.
12. Moreau, D., Cazzolato, B., Zander, A. and Petersen, C., 2008. A review of virtual sensing algorithms for active noise control. *Algorithms,* 1, 69-99.
13. Garcia-Bonito, J., Elliott, S.J. and Boucher, C.C., 1997. Generation of zones of quiet using a virtual microphone arrangement. *Journal of the Acoustical Society of America*, 101 (6), 3498-3516.
14. Kestell, C.D., Cazzolato, B.S. and Hansen, C.H., 2001. Active noise control in a free field with virtual sensors. *Journal of the Acoustical Society of America,* 109 (1), 232-243.
15. Halim, D. Cheng, L. and Su, Z., 2011. Virtual sensors for active noise control in acoustic-structural coupled enclosures using structural sensing: robust virtual sensor design. *Journal of the Acoustical Society of America,* 129 (3), 1390-1399.
16. Roure, A. and Albarrazin, A., 1999. The remote microphone technique for active noise control. In: *Proceedings of the 1999 International Symposium on Active Control of Sound and Vibration (Active 99).* Florida, U.S.A., 04-06 July 1999.
17. Joseph, P., Elliott, S.J. and Nelson, P.A., 1994. Statistical aspects of active control in harmonic enclosed sound fields. *Journal of Sound and Vibration,* 172 (5), 629-655.
18. Elliott, S.J., Maury, C. and Gardionio, P., 2005. The synthesis of spatially correlated random pressure fields. *Journal of the Acoustical Society of America,*117 (3), 1187-1200.
19. Minkoff, J., 1997. The operation of multichannel feedforward adaptive systems. *IEEE Transactions on Signal Processing,* 45 (12), 299-3005.
20. Morari, M. and Zafiriou, E., 1989. *Robust Process Control*, Prentice-Hall.
21. Cheer, J., 2012, *Active Control of the Acoustic Environment in an Automobile Cabin*, PhD Thesis , University of Southampton, Southampton, U.K.
22. Elliott, S.J. and Sutton, T.J., Performance of feedforward and feedback systems for active control, *IEEE Transactions on Speech and Audio Processing*, 4 (3), 214-223.